Engineering of Large Third-Order Nonlinearities in Atomic Layer Deposition Grown Nitrogen-Enriched TiO_2

Robinson Kuis, *,‡,[1,3] Theodosia Gougousi,*, ‡, [2] Isaac Basaldua, [1,3] Paul Burkins,[2,3,4] Jaron A. Kropp,[2] and Anthony M. Johnson[1,2,3]

[1]Department of Computer Science and Electrical Engineering (CSEE), University of Maryland, Baltimore County (UMBC), 1000 Hilltop Circle, Baltimore, Maryland 21250, United States
[2]Department of Physics, University of Maryland, Baltimore County (UMBC), 1000 Hilltop Circle, Baltimore, Maryland 21250, United States
[3]Center for Advanced Studies in Photonics Research (CASPR), University of Maryland, Baltimore County (UMBC), 1000 Hilltop Circle, Baltimore, Maryland 21250, United States
[4]Department of STEM, Harford Community College (HCC), 401 Thomas Run Road, Bel Air, Maryland 21015, United States

ABSTRACT: The third-order nonlinear optical properties of Nitrogen-enriched TiO_2 films deposited by Atomic Layer Deposition (ALD) at a temperature between 100 – 300°C on quartz substrates were studied using thermally managed Z-scan technique. TiO_2 oxide films prepared by Physical Vapor Deposition (PVD) at room temperature were used as control samples. The as-grown ALD films deposited at 150 – 300°C exhibited values for the nonlinear index of refraction, n_2, between $0.6x10^{-11}$ and $1x10^{-9}$ cm^2/W, which is 4–6 order larger than previously reported. Annealing the films, for 3 hours at 450°C in air, reduced the nonlinearities below the detection limit of the experimental setup. Similarly, as-grown 100°C ALD and PVD films did not produce a discernible Z-scan trace. Composition analysis performed by x-ray photoelectrons spectroscopy (XPS) reveals the presence of Ti-O-N metallic bonds in the films that showed high nonlinear optical response. The presence of the metallic bonding gives the films deposited on Si (100) a golden color. These results demonstrate the possibility of a new class of thin-film nonlinear materials that their properties can be tailored by controlling the film composition.

KEYWORDS: nanophotonics, nonlinear optics, thermally managed Z-scan, TiO_2 film, atomic layer deposition, CMOS compatible films

TOC Graphic

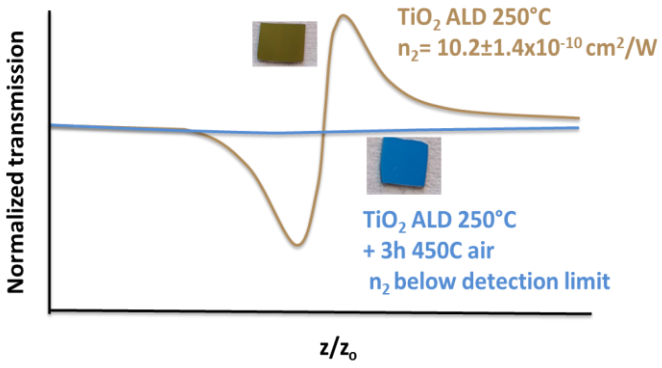
TiO2 ALD 250°C
n2= 10.2±1.4x10-10 cm2/W
TiO2 ALD 250°C
+ 3h 450C air
n2 below detection limit
Normalized transmission
z/z0

Next-generation of high-speed photonics devices, such as ultrafast integrated modulators[1] and wavelength converters,[2] require materials with large third-order optical nonlinearities. Typically, nonlinear materials are cut from bulk crystals or liquids that are not suitable for integration with complementary metal-oxide-semiconductor (CMOS) technology. In addition to all-optical on-a-chip device applications, materials that exhibit high nonlinear absorption and a fast response time are useful in optical limiting applications[3] for the protection of optical sensors and the human eye from high intensity light such as lasers.[4] Previous materials proposed for optical limiting have been semiconductors, fullerenes, carbon nanotubes, nanostructured materials such as nanoparticles, graphene, nonlinear absorbers doped in xerogels and sol-gel films, glasses, filters, organic/inorganic clusters, as well as 2D atomic crystals and organic dye molecules. For most of these materials, there is a tradeoff between their optical limiting ability and damage thresholds, and response time.[5] The vast majority of these materials are not suitable for covering large-scale areas with consistent reproducibly required for sensitive applications such as infrared countermeasures sensors. Therefore, there is a need for CMOS-compatible materials with sizeable nonlinear optical properties.

A potential solution to the scarcity of CMOS-compatible materials is transition-metal oxides (TMOs). These materials have been demonstrated[6] to have large third-order optical nonlinearities with fast response time (~picosecond time scale). Values as large as 8.4×10^{-11} cm^2/W for the nonlinear refractive index (n_2) for a 33.5 nm thick V_2O_5 film have been measured.[6]

In conjunction with having a large and fast nonlinearity, the TMO fabrication process must be compatible with current CMOS technology. There are several techniques, such as atomic layer deposition (ALD), chemical vapor deposition (CVD) and physical vapor deposition (PVD), which are CMOS compatible. However, due to its conformality and control over materials thickness and composition[7-8] ALD is preferred over other deposition methods.

Recent nonlinear optical research has centered on enhancing the second-order nonlinear optical properties by utilizing the monolayer precision of ALD to design nanolaminate films[9-10]. The measurement of the third-order nonlinear properties has been limited to ZnO/Al_2O_3[11-12] and TiO_2/Al_2O_3[12] nanolaminates. It has been shown[13] that ALD grown amorphous TiO_2 films demonstrate large nonlinear refractive index, n_2,(7.2 x10^{-11} cm^2/W) values, which is 4–6 orders larger than what has been reported[14-15] previously. In addition, annealing the films in an air rich environment reduces the nonlinearity to levels below the detection limit of the experimental Z-scan setup. The results suggest that the initial condition during fabrication in combination with annealing could be used to control the third-order nonlinearity of the films.

In this paper, we report on the potential cause of the augmentation to the nonlinearity. X-ray photoelectron spectroscopy (XPS) revealed that the TiO_2 films showing high nonlinearities have, during the fabrication process, incorporated nitrogen in the form of Ti-O-N bonds. An enhancement of 6 orders for films grown at 250°C resulted from about 1 at. % of Ti-O-N bonds evenly distributed within the films. The small density of bonds dramatically increases the film's absorption across the visible to the near-infrared spectrum (350 – 900 nm). The XPS data allowed the correlation of high nonlinear optical response with the presence of Ti-O-N bonding in the films.

EXPERIMENTAL APPROACH

Sample preparation. TiO_2 ALD films, with 60 nm nominal thickness were deposited at 100, 150, 200, 250, 275 and 300°C on quartz and native oxide Si(100) concurrently using thermal ALD with tetrakis dimethylamino titanium (TDMAT) and H_2O.[16, 17] For our reactor configuration 200°C is the optimal ALD temperature. The nominal film thickness was based on the process growth rate per cycle derived by measuring the thickness of thinner films deposited on native oxide Si (100)

using spectroscopic ellipsometry (Woollam alsphaSE). Because of the process conformality, both sides of the glass substrate were coated resulting in an effective film thickness of 120 nm when tested in transmission. ALD films were also grown on a single side of the substrate by masking one side. 100 nm PVD TiO_2 films were also deposited from a 99.9% TiO_2 target at room temperature (RT) and used as control samples. All glass substrates were cleaned by immersion in acetone (5 min), and methanol (5 min) followed by deionized (DI) water rinse (5 min) and blown dry with N_2. Native oxide Si (100) substrates were cleaned by immersion in JT Baker (100) for 5 min, DI water rinse (5 min) and blown dry by N_2. Films were annealed at 450°C for 3 hrs in the ambient atmosphere in a furnace (Fisher Isotemp 750 Series). The temperature was ramped up at 15°C/min and after the 3 hrs soak at 450°C the films were allowed to cool down in ambient.

Nonlinear optical properties evaluation. Z-scan is an established and very versatile laser-based technique that allows for the measurement of both the sign and magnitude of the nonlinear refractive index (n_2) of a material with a level of sensitivity comparable to interferometric methods.

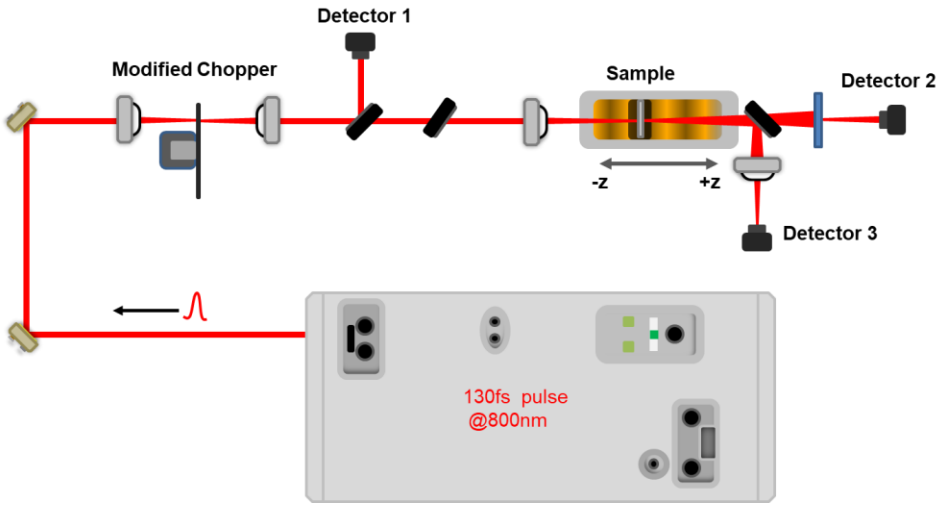

Figure 1. Diagram of thermally-managed Z-scan setup[19] used in the nonlinear measurements. The setup shows the modified optical chopper, 800 nm 130 fs laser system, reference, CA and OA detectors, various focusing lenses and sample translation stage.

Additionally, it allows the indirect measurement of the nonlinear absorption coefficient (β). There are two components to Z-scan (see Figure 1), closed aperture (CA) and open aperture (OA). The CA Z-scan technique yields the n_2, while the OA Z-scan yields the nonlinear absorption of the material. Procedurally, the Z-scan setup makes use of three photodetectors. One photodetector (Detector 1) measures the light prior to entering the sample (reference) and the other two detects the Z-scan signal, one for OA (Detector 3) and one for CA (Detector 2). Dividing the signal by the reference effectively eliminates laser power fluctuations from the data. The Z-scan trace data is produced as the sample is moved in and out of the lens focus. The OA Z-scan produces a trace that has a peak and valley at particular positions. The order of the appearance of either peak then valley (negative nonlinearity) or valley then peak (positive nonlinearity) depends on the sign of the non-linearity. The transmission for the OA and CA Z-scan is given by [18]

$$T_{CA}(z) = 1 - \frac{4\Delta\phi_0 \frac{z}{z_0}}{\left[\left(\frac{z}{z_0}\right)^2 + 9\right]\left[\left(\frac{z}{z_0}\right)^2 + 1\right]}, \quad (1)$$

and

$$T_{OA}(z) = \frac{1}{q_o\sqrt{\pi}} \int_{-\infty}^{\infty} \ln\left(1 + q_0 e^{-t^2}\right) dt, \quad (2)$$

where z is the sample position, z_o is the Rayleigh range, $\Delta\phi_0$ is the phase shift due to the nonlinearity and is given by $\Delta\phi_0 = k n_2 I_0(t) L_{eff}$ and k ($=2\pi/\lambda$) is the propagation constant and L_{eff} ($= (1 - e^{-\alpha L})/\alpha$, where α is the linear absorption coefficient and L is the sample path length) is the effective path length of the sample, and q_0 (z, t) = $\beta I_0(t) L_{eff}$.

For a high repetition laser, such as the 76 MHz, 130 fs Ti: sapphire laser used in this work, it has been determined that unwanted thermal effects can accumulate, which can be managed by using a modified mechanical chopper[19-20] or pulse picker. This effectively lowers the repetition rate and

allows the sample to cool between bursts or groups of pulses, allowing the extraction of the electronic nonlinear optical properties of the sample. Calibration of the Z-scan setup was conducted using the well-known liquid CS_2 (see calibration results in supporting information) as described by Sheik-Bahae[18]and Burkins[19]. The measured n_2 value of CS_2 was $2.48\pm0.1\times10^{-15}cm^2/W$ which is close to the excepted value of $2.4\times10^{-15}cm^2/W$.[18] At the full repetition rate of the laser, the n_2 value appears negative due to the thermal effects while at the thermally managed repetition rate a positive value is obtained as measured using low repetition lasers. These calibration measurements give us great confidence in our measurement capability.

The Z-scan measurements were all performed using the modified chopper.[19-20] The modified chopper has a small single slit (< 1 mm in width) and is placed at the focus of a telescope (see Figure 1) to prevent any loss in power. The laser was focused with a 7.5 cm focal length lens which produces a focal spot diameter of 13.1 μm at the sample. The peak irradiance used to measure the samples varied from 13.2 GW/cm^2 to 145.5 GW/cm^2 (equivalent to peak fluence range of 1.95 mJ/cm^2 to 21.5 mJ/cm^2) depending on the sample under test.

It has been shown that damage on the surfaces of films[21] and optical cuvettes[22] can produce Z-scan traces that appear to result in large optical nonlinearities. To investigate this possibility, Z-scan measurements were also performed on various locations on the samples' surface and also on duplicate samples. Conducting these measurements provide confidence that the Z-scan results were not due to damage spots caused by the focused laser beam. The results from these measurements were consistent (within 10% of each other), which reflect the uniformity of the ALD growth process.

Potential etalon effects were evaluated for the one and two-sided samples prepared for the optical measurements; tilting the films slightly demonstrated a reduction in such an effect. The nonlinear

measurements showed no significant difference in the nonlinear properties between the single and double-sided films. The experiments, therefore, continued with samples having films on both sides since it provided a longer path length for the nonlinear measurements.

Characterization of TiO_2 films. The composition of the TiO_2 films was characterized by XPS using a Kratos AXIS 165 spectrometer equipped with an Al monochromatic X-ray source (1486.6 eV) and a hemispherical analyzer (165 mm radius). High-resolution spectra were recorded using a 20 eV pass energy at 0.1 eV step size. Charge compensation was performed by placing the C 1s peak at 484.5 eV. Films were examined without sputtering the topmost layer except for the two samples used for depth profiling. The film structure was obtained by XRD using a D8 Advance diffractometer with Cu Kα x-ray source (λ = 1.54 Å). Film transmission was measured using a JASCO V570 (200 – 2500 nm) UV-Vis spectrometer.

RESULTS AND DISCUSSION

The third-order nonlinearity for the as-deposited and thermally treated TiO_2 ALD films prepared at six different temperatures was examined using Z-scan. PVD TiO_2 films deposited at room temperature were used as control samples. Figure 2 shows sample CA Z-scan results for the as-deposited 150ºC and 250°C ALD films, 250°C annealed ALD film, and control PVD TiO_2 film deposited on the quartz substrate. Z-scan measurements of the as-deposited 250°C film utilized 300mW of average power and produced the largest n_2 value ($10.2\pm1.4\times10^{-10}$ cm^2/W). The power was doubled (600mW) to evaluate the potential power dependence of the nonlinearity. Z-scan traces of the 250°C film at this power scaled linearly as compared to traces at lower power. The 150°C film required an average power of 900 mW produced a Z-scan trace and the film had the smallest n_2 ($0.59\pm0.05\times10^{-10}$ cm^2/W) measured. For the PVD grown TiO_2 film as well as the thermally treated (3 hours, 450°C in an air) version of the film 250°C film, the Z-scan

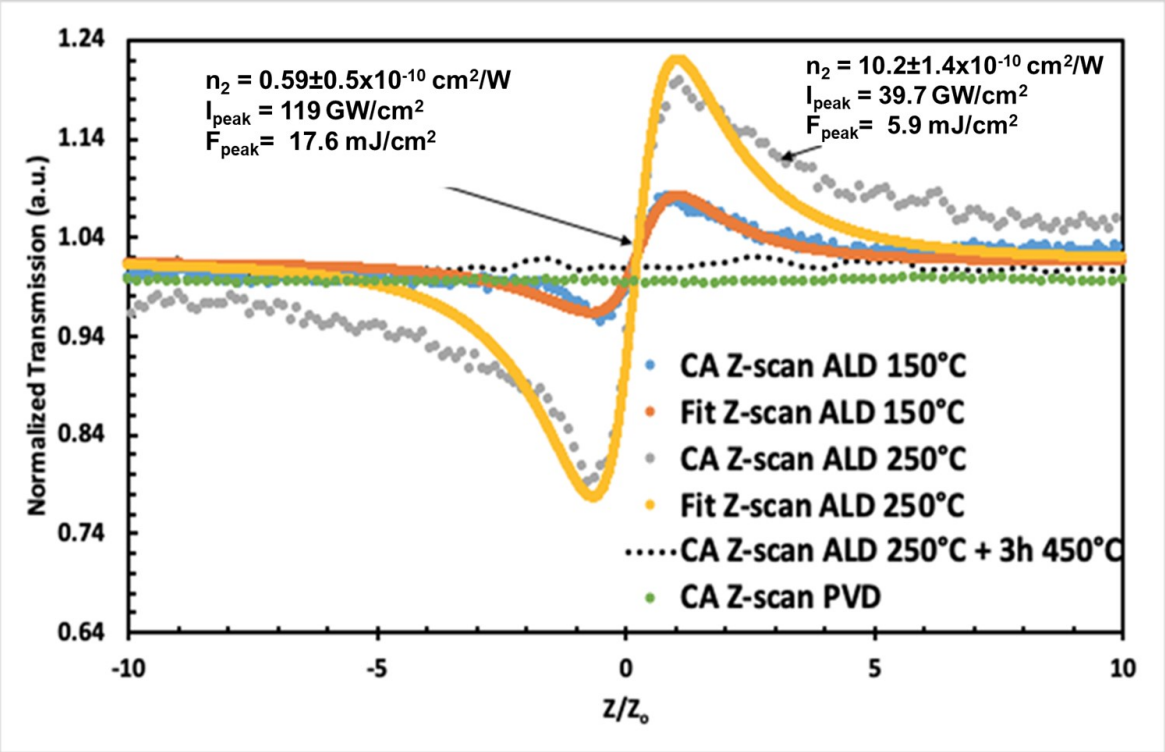

Figure 2. Z-scan results for ALD TiO_2 samples deposited at 150°C (at irradiance of 119 GW/cm^2), and 250°C (at irradiance of 39.7 GW/cm^2), the thermally treated 250°C sample (at irradiance of 132 GW/cm^2) and the PVD TiO_2 control sample (at irradiance of 132 GW/cm^2). Both the thermally treated and the control sample produced responses below detection limits.

measurements were carried at the maximum laser average power (1300 mW). Even at such high power, the nonlinear phase shifts produced by these films were too small and the traces appear as nearly straight horizontal lines in Figure 2. The measured n_2 for all ALD and control film samples is summarized in Table 1. The as-grown 200ºC, 275ºC and 300°C films produced measured n_2 values of 5.2 ± 0.3x10^{-10} cm^2/W, 7.3±0.5x10^{-10} cm^2/W, and 8±0.63x10^{-10} cm^2/W respectively. The ALD films grown at 275ºC and 300°C have similar - within the error of the measurement n_2 values. The 100°C as-grown ALD film shows a response below the detection limit of our Z-scan measurement. After thermal treatment, the Z-scan measurements for all ALD films produced no discernable phase shift up to the maximum available power from the laser system. The nonlinear

properties of TiO_2 have been tested in detail[14-15,23] and tend to show values for the n_2 of 4-6 order smaller than the value reported here. The fact that thermal treatment in an oxygen-rich atmosphere

Table 1. Measured n_2 values for the various TiO_2 films examined in this work including the peak irradiance used at each Z-scan measurement.

Material	λ_o(nm)	I_{peak} (GW/cm^2)	n_2(cm^2/W)
CS_2 (liq.)	800	145.5	$2.48\pm0.1\times10^{-15}$
"TiO_2" ALD 100°C	800	132	< detection limit
"TiO_2" ALD 150°C	800	119	$0.59\pm0.05\times10^{-10}$
"TiO_2" ALD 200°C	800	39.7	$5.2\pm0.33\times10^{-10}$
"TiO_2" ALD 250°C	800	39.7	$10.2\pm1.4\times10^{-10}$
"TiO_2" ALD 275°C	800	39.7	$7.3\pm0.5\times10^{-10}$
"TiO_2" ALD 300°C	800	39.7	$8\pm0.63\times10^{-10}$
"TiO_2" ALD +3h 450°C air	**800**	**132**	**< detection limit**
TiO_2PVD RT	800	132	< detection limit

leads to the loss of the nonlinear response for all samples indicates that the measured nonlinear response is due to a structural or compositional "peculiarity" in the as-deposited films.

Optical images for some of the samples deposited on Si (100) surfaces are shown in Figures 3(a) and (b). While all ALD films are of similar thickness, there is a marked difference in their color. The as-grown films at 200ºC to 300°C have a golden metallic color. The film prepared at 100°C is a dark shade of blue while the one prepared at 150°C looks golden purple. After thermal treatment, all the ALD films prepared at 150°C and higher temperatures turn a shade of blue. For comparison, the PVD TiO_2 films is also a very light shade of blue.

These results already point to the presence of some differences in the films. This is not unexpected as a variation of the ALD process temperature is known to result in variation in the film carbon and water content. Films deposited at 100°C are known to contain a substantial amount of water and carbon. Films prepared at 200ºC and 250°C have been shown to be the purest and with very

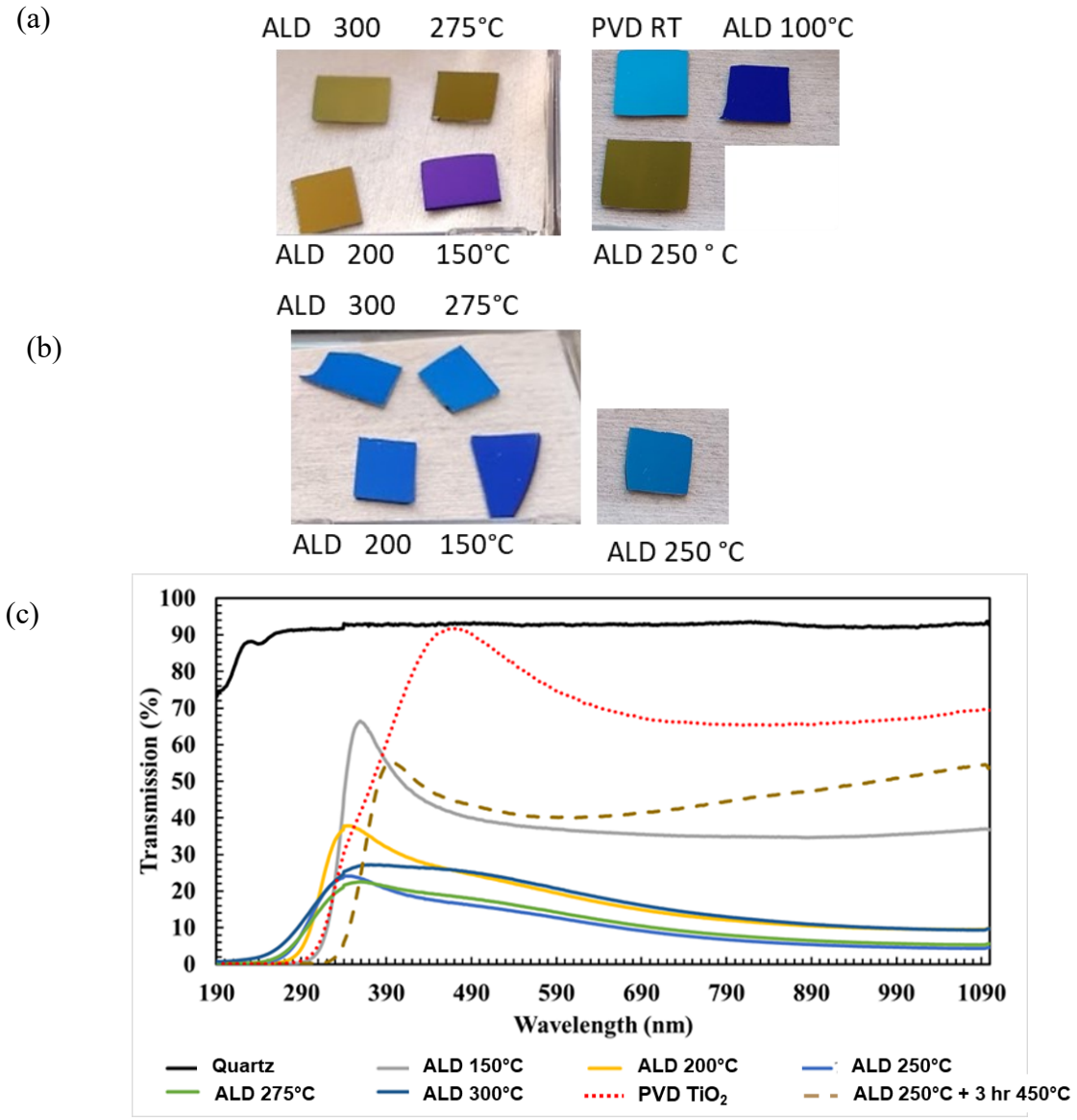

Figure 3. Optical images for the some of TiO_2 ALD and PVD films on native oxide Si (100) (a) as-deposited, (b) after thermal treatment for 3hrs, 450°C in air and (c) Transmission measurements for a set of ALD TiO_2 films, PVD TiO_2 film, and substrate (quartz) examined in this work.

similar composition.[17] This difference in color is also mirrored in the difference in the film transmission (Figure 3(c)). Before annealing, the transmission for the as-grown 250°C TiO_2 film was

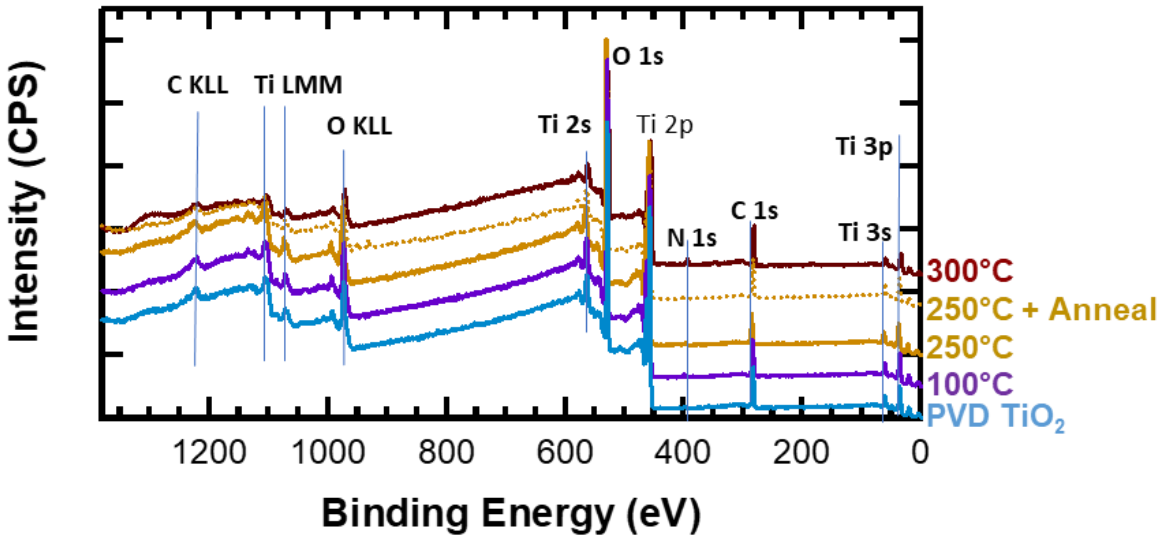

Figure 4. Survey XP spectra for some of the films investigated in this work. All films are TiO_2 with varying concentrations of carbon and nitrogen containing impurities.

7% while after annealing increased to 46.6%. For the case of the 100°C as-grown film, transmission before and after annealing only changed marginally from 52.5% to 54%. For the as-deposited ALD films it appears that the onset of absorption is blue-shifted unlike nitrogen-containing TiO_2 films produced by other techniques. [24–26] For the ALD 250°C film there is a marked red-shift of the bandgap after thermal treatment.

To investigate the potential differences in film composition, all films were examined using X-ray photoelectron spectroscopy (XPS) and the survey spectra for some of the films are shown in Figure 4. All the films are composed of Ti and O. Carbon in both adventitious and bonded form is the main impurity and nitrogen originating from the amine precursor is also detected in some of the films.

Figures 5a and 5b show high-resolution XP spectra for the Ti 2p and C 1s regions for several samples. Sample fits for the C 1s and Ti 2p spectra are shown in the supporting information. The

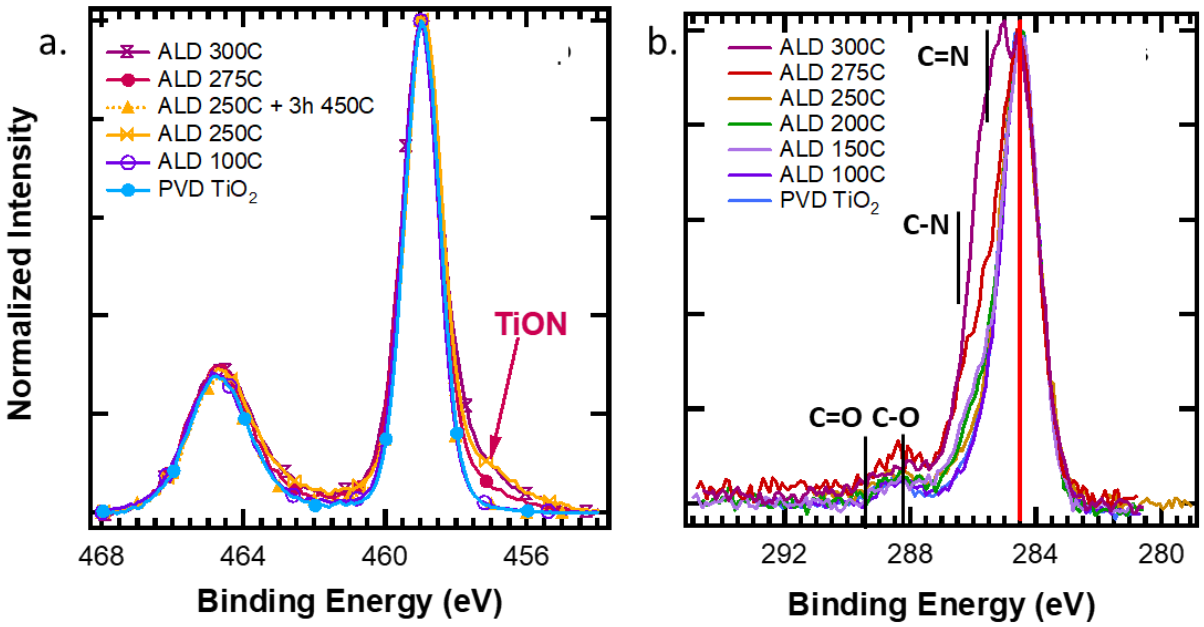

Figure 5. (a) Ti 2p and (b) C 1s high resolution XP spectra for some of the films examined in this work. For the films that exhibit high n_2 value, a shoulder is detected in the Ti 2p spectra that is compatible with the presence of Ti-O-N bonding. Carbon containing impurities are detected for all films. The one deposited at temperatures above the ALD window contain the largest concentration of such impurities.

as-deposited samples at 250ºC, 275ºC, and 300°C all exhibit high nonlinear response and in the Ti 2p region a small shoulder is observed around 457.5 eV. This shoulder is absent both for the 100°C ALD sample, the PVD sample, and all thermally treated samples. A couple of different assignments are possible for this feature so information from other regions is required to make a definitive peak assignment. The C 1s region shows the presence of bonded carbon mainly in C-N form (286.5 eV) indicating the presence of precursor ligands.[27] Films deposited at 275ºC and 300°C show the highest concentration of such bonding, compatible with films produced under quasi CVD conditions.

The N 1s region (Fig 6a) reveals the presence of a peak that is compatible with Ti-N-O bonding only for the as-deposited 250ºC, 275ºC and 300°C ALD films, the films that show the highest nonlinear response and also exhibit the shoulder in the Ti 2p spectra.[28] When the films were thermally treated in an oxygen-rich environment, this peak disappeared from the spectra resulting in the reduction of the nonlinear response. Ti-N is known to oxidize easily so we expect that the Ti-N-O bonding was converted to Ti-O and N-O bonding. The presence of N-O bonding is confirmed by the peak appearing in the 275ºC and 300°C thermally treated films at ~402 eV.[27] TiN is a refractory metal with a characteristic golden color and this is evident in the optical images in Figure 3(a). Composition analysis indicates that the N contained in the films in this type of bonding ranges from 0.7 at.% for the 250°C sample to ~2.6 at.% for the 300°C sample. We cannot determine accurately the at.% of such bonding for the 150ºC and 200°C samples due to selective removal of O from the films.[29] [30] From the peak height for the relevant N1s peak one can conclude that it is less than that for the 250°C sample.

The as-deposited films at 150ºC and 200°C also showed moderately high nonlinearity however the N 1s did not show the presence of the Ti-O-N peak. As mentioned before, TiN is known to oxidize upon ambient exposure, so depth profiling was performed to investigate the presence of such bonding in the film bulk and these results are shown in Figures 6b and c. Indeed, the presence of Ti-O-N is confirmed for both of these films. The 200°C shows a higher concentration of this type of bonding and this translates to a higher measured value for n_2. This direct correlation does not hold for the samples deposited at the higher end of the temperature range as the 300°C sample has the highest peak associated with the Ti-O-N but shows somewhat smaller n_2 than the 250°C sample. The 300°C sample also has the largest concentration of C-containing impurities, so it is

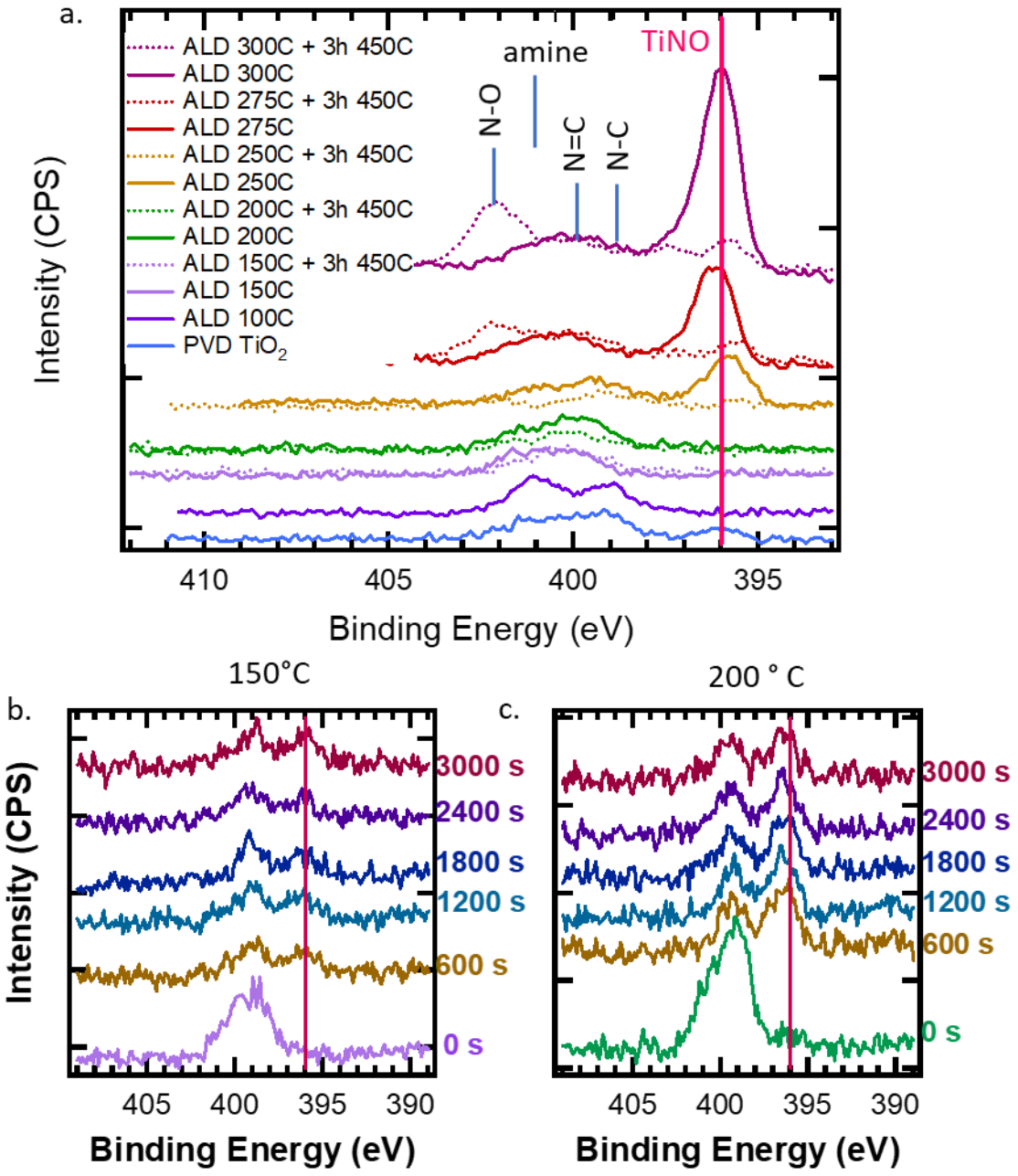

Figure 6. (a). N1s high resolution XPS data for the ALD TiO_2 films deposited at temperatures ranging from 100ºC to 300°C and room temperature PVD TiO_2 films, (b) and (c). N 1s depth profiles for ALD TiO_2 films deposited ta 150ºC and 200°C respectively.

conceivable that there is "cancellation" of the beneficial effect of the Ti-N bonding from the presence of other impurities.

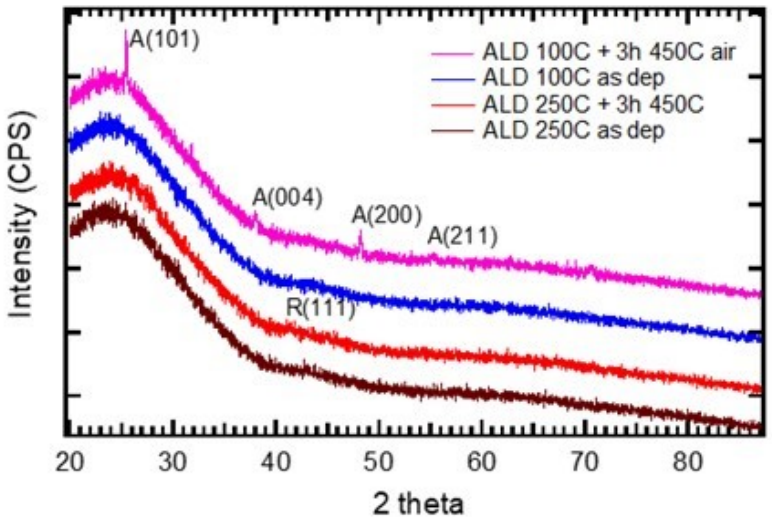

Figure 7. X-ray diffraction data for the ALD TiO_2 films deposited at 100°C and 250°C.

X-ray Diffraction analysis of some of the ALD samples indicates that the as-grown films are amorphous and remain practically amorphous even after the thermal treatment (Figure 7). The annealed 100°C ALD film shows a couple of peaks compatible with the presence of anatase crystallites in agreement with earlier observations[17]. A change in the sample degree of crystallization can thus be excluded as the source of the nonlinear properties.

The cause of the nonlinearity can be understood as follows. The presence of Ti-N-O bonding in the golden colored films which is metallic in nature results in a drastic increase in the absorption. The increase of absorption may be counterintuitive since the films are more metallic and their reflective properties should increase. Therefore, experiments were conducted to evaluate the reflection of the as-grown and annealed 250°C films. Unfocused light (2-3 mm diameter spot) at an 800 nm wavelength was incident on the films. The films were placed in a rotational stage that enables the placement of an angle between the films and the incident beam. A power meter was used to measure the transmitted and reflected powers from films at an angle of 1°. The percentage

of the transmitted and reflected powers were calculated by dividing these quantities by the incident power. The transmitted power for the 250°C as-grown (ALD 250C) and annealed (ALD 250C + 3 h 450C) are 7% and 28%, respectively. The reflected powers for the same films are 48% and 52% respectively. Clearly, the measurement shows that the as-deposited samples absorb more light than their annealed counterparts. TiO_2, in general, is known to be an n-type semiconductor[31]. Typically, for off-resonance or low-loss dielectrics, the nonlinear index of refraction, n_2, (assuming Kerr-type nonlinear response) is related to the real part of the nonlinear susceptibility, $\chi_R^{(3)}$, by [32]

$$n_2 = \frac{3}{4n_o^2\varepsilon_o c}\chi_R^{(3)}, \tag{3}$$

where n_0 is the linear refractive index, ε_0, in the electric permittivity of free space, and c is the speed of light in vacuum. In the case of on resonance and or absorbing media (metallic-like films), the nonlinear index becomes:[33,34]

$$n_2 = \frac{3}{4(n_o^2+k_0^2)\varepsilon_o c}\left[\chi_R^{(3)} + \frac{k_0}{n_0}\chi_I^{(3)}\right], \tag{4}$$

where k_0 is the linear absorption index and is related to the absorption coefficient ($k_0 = \lambda\alpha/4\pi$), and $\chi_I^{(3)}$ is the imaginary part of the third-order nonlinear susceptibility. Like metallic films, the increased nonlinear properties of the films will depend on the linear absorption. This result is illustrated in Table 2, where the relation between the measured nonlinear index of refraction at 800 nm and the calculated linear absorption index is shown. The increase in absorption correlates with the increase in the nonlinear index of refraction as predicted by equation (4). Controlling the deposition temperature can control the percentage of Ti-O-N bond present in the film and simultaneously control the nonlinearity. In addition, post-deposition control of the nonlinear properties can

also be done by annealing the films. Annealing effectively removes any created Ti-O-N bond during fabrication as well as the absorption.

CONCLUSIONS

Some ALD TiO_2 films deposited from TDMAT and H_2O show very high nonlinear optical response. Thermal treatment of these films in an air environment for 3 hours at 450°C quenches this response completely. The measured nonlinear index of refraction n_2 for these films is orders of magnitude higher than that for CS_2, which is a standard and well-known nonlinear optical material. The ALD process temperature is shown to have a substantial effect on the film nonlinear response. The variation of the deposition temperature leads to a significant variation in the Ti-N-O content of the films. Thermal treatment removes such bonding from the films and results in the loss of the nonlinear response. The coupling between the Ti-N at.% content of the film and its measured n_2 is not a linear relationship indicating that there may be other parameters that influence its nonlinear optical response.

Table 2. The relation between the linear absorption index $k_0 = \lambda\alpha/4\pi$ and the nonlinear index for the ALD films.

Growth Temp. (°C)	Linear Absorption Index, k_0	Nonlinear Index, n_2 (10^{-10}cm^2/W)
100	0.34	Below detection limit
150	0.55	0.59±0.05
200	1.12	5.2±.33
250	1.44	10.2±1.4
275	1.35	7.3±0.5
300	1.09	8±0.63
100(annealed)	0.35	Below detection limit
150(annealed)	0.37	Below detection limit
200(annealed)	0.43	Below detection limit
250(annealed)	0.43	Below detection limit
275(annealed)	0.37	Below detection limit
300(annealed)	0.28	Below detection limit

AUTHOR INFORMATION

Corresponding Authors

* E-mail: Robinson.kuis@umbc.edu.

* Email: gougousi@umbc.edu

Author Contributions

‡ These two authors contributed equally**.** The manuscript was written through contributions of all authors. All authors have given approval to the final version of the manuscript.

Notes

The authors declare no competing financial interest.

ACKNOWLEDGMENTS

We thank the UMBC START program for providing seed funding. We thank Dr. Lisa Kelly, Dr. Brad Arnold, and Ms. Stacey Sova from the Department of Chemistry & Biochemistry (UMBC) for their assistance in obtaining the transmission data of the films, and Dr. Karen Gaskell at the University of Maryland for taking the XPS data. This material is based upon work supported by the National Science Foundation under grants ECCS-1407677 and DMR-1905305.

SUPPORTING INFORMATION

Supporting Information Available: Sample Ti 2p and C 1s high-resolution XPS scans, associated fits, and calibration results of Z-scan setup with CS_2**.** (Figures S1, S2, and S3) This material is available free of charge via the Internet at http://pubs.acs.org

REFERENCES

(1) Yang, S.; Liu, D. C.; Tan, Z. L.; Liu, K.; Zhu, Z. H.; Qin, S. Q. CMOS-Compatible WS2-Based All-Optical Modulator. *ACS Photonics* **2018**, *5* (2), 342–346. https://doi.org/10.1021/acsphotonics.7b01206.

(2) C. Lacava; L. Carrol; A. Bozzola; R. Marchetti; P. Minzioni; I. Cristiani; M. Fournier; S. Bernabe; D. Gerace; L. C. Andreani. Design and Characterization of Low-Loss 2D Grating Couplers for Silicon Photonics Integrated Circuits; 2016; Vol. 9752, pp 97520V-9752–9757.

(3) Dini, D.; Calvete, M. J. F.; Hanack, M. Nonlinear Optical Materials for the Smart Filtering of Optical Radiation. *Chem. Rev.* **2016**, *116* (22), 13043–13233. https://doi.org/10.1021/acs.chemrev.6b00033.

(4) G. Ritt; S. Dengler; B. Eberle. Protection of Optical Systems against Laser Radiation. In *Proc. SPIE 7481*; 2009; Vol. 7481, pp 74810U-7481–7489.

(5) Khurgin, J. B. Response to "Comment on 'Graphene—A Rather Ordinary Nonlinear Optical Material'" [Appl. Phys. Lett. 111, 106101 (2017)]. *Appl. Phys. Lett.* **2017**, *111* (10), 106102. https://doi.org/10.1063/1.4999183.

(6) Ando, M.; Kadono, K.; Haruta, M.; Sakaguchi, T.; Miya, M. Large Third-Order Optical Nonlinearities in Transition-Metal Oxides. *Nature* **1995**, *374*, 625.

(7) Johnson, R. W.; Hultqvist, A.; Bent, S. F. A Brief Review of Atomic Layer Deposition: From Fundamentals to Applications. *Materials Today* **2014**, *17* (5), 236–246. https://doi.org/10.1016/j.mattod.2014.04.026.

(8) Hausmann, D. M.; de Rouffignac, P.; Smith, A.; Gordon, R.; Monsma, D. Highly Conformal Atomic Layer Deposition of Tantalum Oxide Using Alkylamide Precursors. *Thin Solid Films* **2003**, *443* (1), 1–4. https://doi.org/10.1016/S0040-6090(03)00502-9.

(9) Alloatti, L.; Kieninger, C.; Froelich, A.; Lauermann, M.; Frenzel, T.; Köhnle, K.; Freude, W.; Leuthold, J.; Wegener, M.; Koos, C. Second-Order Nonlinear Optical Metamaterials: ABC-Type Nanolaminates. *Appl. Phys. Lett.* **2015**, *107* (12), 121903. https://doi.org/10.1063/1.4931492.

(10) Wickberg, A.; Kieninger, C.; Sürgers, C.; Schlabach, S.; Mu, X.; Koos, C.; Wegener, M. Second-Harmonic Generation from ZnO/Al2O3 Nanolaminate Optical Metamaterials Grown by Atomic-Layer Deposition. *Advanced Optical Materials* **2016**, *4* (8), 1203–1208. https://doi.org/10.1002/adom.201600200.

(11) Karvonen, L.; Säynätjoki, A.; Chen, Y.; Jussila, H.; Rönn, J.; Ruoho, M.; Alasaarela, T.; Kujala, S.; Norwood, R. A.; Peyghambarian, N.; et al. Enhancement of the Third-Order Optical Nonlinearity in ZnO/Al2O3 Nanolaminates Fabricated by Atomic Layer Deposition. *Appl. Phys. Lett.* **2013**, *103* (3), 031903. https://doi.org/10.1063/1.4813557.

(12) Lasse Karvonen; Tapani Alasaarela; Henri Jussila; Soroush Mehravar; Ya Chen; Antti Säynätjoki; Robert A. Norwood; Nasser Peyghambarian; Khanh Kieu; Seppo Honkanen; et al. Nanolaminate Structures Fabricated by ALD for Reducing Propagation Losses and Enhancing the Third-Order Optical Nonlinearities. In *Proc. SPIE*; 2014; Vol. 8982, pp 89820O-8982–8989.

(13) Burkins, P. Femtosecond Z-Scan Measurements in Novel Materials with Emphasis on Managing Thermal Effects, University of Maryland, Baltimore County, Baltimore, Maryland, 2017.
(14) Portuondo-Campa, E.; Tortschanoff, A.; van Mourik, F.; Chergui, M. Ultrafast Nonresonant Response of TiO2 Nanostructured Films. *The Journal of Chemical Physics* **2008**, *128* (24), 244718. https://doi.org/10.1063/1.2949517.
(15) Das, S. K.; Schwanke, C.; Pfuch, A.; Seeber, W.; Bock, M.; Steinmeyer, G.; Elsaesser, T.; Grunwald, R. Highly Efficient THG in TiO2 Nanolayers for Third-Order Pulse Characterization. *Opt. Express* **2011**, *19* (18), 16985–16995. https://doi.org/10.1364/OE.19.016985.
(16) Hackley, J. C.; Gougousi, T.; Demaree, J. D. Nucleation of HfO2 Atomic Layer Deposition Films on Chemical Oxide and H-Terminated Si. *Journal of Applied Physics* **2007**, *102* (3), 034101. https://doi.org/10.1063/1.2764223.
(17) Henegar, A. J.; Gougousi, T. Stability and Surface Reactivity of Anatase TiO2 Films. *ECS J. Solid State Sci. Technol.* **2015**, *4* (8), P298–P304. https://doi.org/10.1149/2.0041508jss.
(18) Sheik-bahae, M.; Said, A. A.; Van Stryland, E. W. High-Sensitivity, Single-Beam N2 Measurements. *Opt. Lett.* **1989**, *14* (17), 955–957. https://doi.org/10.1364/OL.14.000955.
(19) Burkins, P.; Kuis, R.; Basaldua, I.; Johnson, A. M.; Swaminathan, S. R.; Zhang, D.; Trivedi, S. Thermally Managed Z-Scan Methods Investigation of the Size-Dependent Nonlinearity of Graphene Oxide in Various Solvents. *J. Opt. Soc. Am. B* **2016**, *33* (11), 2395–2401. https://doi.org/10.1364/JOSAB.33.002395.
(20) Falconieri, M.; Salvetti, G. Simultaneous Measurement of Pure-Optical and Thermo-Optical Nonlinearities Induced by High-Repetition-Rate, Femtosecond Laser Pulses: Application to CS2. *Applied Physics B* **1999**, *69* (2), 133–136. https://doi.org/10.1007/s003400050785.
(21) Patterson, B. M.; White, W. R.; Robbins, T. A.; Knize, R. J. Linear Optical Effects in Z-Scan Measurements of Thin Films. *Appl. Opt.* **1998**, *37* (10), 1854–1857. https://doi.org/10.1364/AO.37.001854.
(22) Edziah, R.; Lalanne, E.; Torres, V.; Johnson, A. M.; Trivedi, S. Z-Scan Measurements Using Ultrashort High-Repetition-Rate Lasers: How to Recognize the Parasitic Effects of Nonlinear Behavior of Fused-Silica Damage Sites. *J. Opt. Soc. Am. B* **2011**, *28* (6), 1385–1390. https://doi.org/10.1364/JOSAB.28.001385.
(23) C.C. Evans. Nonlinear Optics in Titanium Dioxide: From Bulk to Integrated Optical Devices Doctoral Dissertation, Harvard, 2013.
(24) Delegan, N.; Daghrir, R.; Drogui, P.; El Khakani, M. A. Bandgap Tailoring of *in-Situ* Nitrogen-Doped TiO $_2$ Sputtered Films Intended for Electrophotocatalytic Applications under Solar Light. *Journal of Applied Physics* **2014**, *116* (15), 153510. https://doi.org/10.1063/1.4898589.
(25) Wu, P.-G.; Ma, C.-H.; Shang, J. K. Effects of Nitrogen Doping on Optical Properties of TiO2 Thin Films. *Applied Physics A* **2005**, *81* (7), 1411–1417. https://doi.org/10.1007/s00339-004-3101-4.
(26) Chen, S.; Zhu, Y. Y.; Xu, R.; Wu, Y. Q.; Yang, X. J.; Fan, Y. L.; Lu, F.; Jiang, Z. M.; Zou, J. Superior Electrical Properties of Crystalline Er2O3 Films Epitaxially Grown on Si Substrates. *Applied Physics Letters* **2006**, *88* (22), 222902. https://doi.org/10.1063/1.2208958.
(27) Papakonstantinou, P.; Lemoine, P. Influence of Nitrogen on the Structure and Nanomechanical Properties of Pulsed Laser Deposited Tetrahedral Amorphous Carbon. *J. Phys.: Condens. Matter* **2001**, *13* (13), 2971–2987. https://doi.org/10.1088/0953-8984/13/13/311.

(28) Song, X.; Gopireddy, D.; Takoudis, C. G. Characterization of Titanium Oxynitride Films Deposited by Low Pressure Chemical Vapor Deposition Using Amide Ti Precursor. *Thin Solid Films* **2008**, *516* (18), 6330–6335. https://doi.org/10.1016/j.tsf.2007.12.148.
(29) Choudhury, T.; Saied, S. O.; Sullivan, J. L.; Abbot, A. M. Reduction of Oxides of Iron, Cobalt, Titanium and Niobium by Low-Energy Ion Bombardment. *Journal of Physics D: Applied Physics* **1989**, *22* (8), 1185–1195. https://doi.org/10.1088/0022-3727/22/8/026.
(30) Ratner, B. D.; Castner, D. G. Electron Spectroscopy for Chemical Analysis. In *Surface Analysis – The Principal Techniques*; John Wiley & Sons, Ltd, 2009; pp 47–112. https://doi.org/10.1002/9780470721582.ch3.
(31) Iancu, A. T.; Logar, M.; Park, J.; Prinz, F. B. Atomic Layer Deposition of Undoped TiO2 Exhibiting P-Type Conductivity. *ACS Appl. Mater. Interfaces* **2015**, *7* (9), 5134–5140. https://doi.org/10.1021/am5072223.
(32) Boyd, R. W. *Nonlinear Optics, Third Edition*; Academic Press, Inc., 2008.
(33) del Coso, R.; Solis, J. Relation between Nonlinear Refractive Index and Third-Order Susceptibility in Absorbing Media. *J. Opt. Soc. Am. B* **2004**, *21* (3), 640–644. https://doi.org/10.1364/JOSAB.21.000640.
(34) Smith, D. D.; Yoon, Y.; Boyd, R. W.; Campbell, J. K.; Baker, L. A.; Crooks, R. M.; George, M. Z-Scan Measurement of the Nonlinear Absorption of a Thin Gold Film. *Journal of Applied Physics* **1999**, *86* (11), 6200–6205. https://doi.org/10.1063/1.371675.